Quantum entanglement manifestation of transition to nonlinear self-trapping for Bose-Einstein condensates in a symmetric double well

L. Fu and J. Liu*

Institute of Applied Physics and Computational Mathematics, P. O. Box 8009 (28), 100088 Beijing, China

(Received 18 September 2006; published 13 December 2006)

We investigate the nonlinear self-trapping phenomenon of a Bose-Einstein condensate (BEC) in a symmetric double well, emphasizing its underlying dynamical phase transition. As the nonlinear parameter characterizing the interaction between the degenerate atoms increases, the BEC becomes self-trapped, manifesting an asymmetric distribution of the atomic density profile. The essence of this phenomenon is revealed to be a continuous phase transition and the underlying critical behavior is studied analytically and found to follow a logarithmic scaling law. We then go beyond the mean-field treatment and extend our treatment to discuss the effect of many-body quantum fluctuations on the transition. It is found that the transition point is shifted and the scaling law is broken. In particular, the quantum phase transition is accompanied by a change of the entanglement entropy, which is found to reach a maximum at the transition point. The underlying physics is revealed.

DOI: 10.1103/PhysRevA.74.063614 PACS number(s): 03.75.Gg, 68.35.Rh

I. INTRODUCTION

The double-well system is a paradigm used to demonstrate quantum tunneling [1]. The realization of a dilute Bose degenerate gas in the 1990s provides the possibility of directly observing the tunneling in a matter wave of macroscopic scale up to 100 μm [2]. In Bose-Einstein condensates (BECs) the interaction between the degenerate ultracold atoms plays a crucial role. It dramatically affects the quantum dynamics and leads to many unusual phenomena like nonlinear Josephson oscillation, nonlinear quantum tunneling, and critical onset of coherent oscillations, etc. [3–6]. These problems have attracted much theoretical attention over the past few years and the recent realization of BECs in the optical trap of a double-well configuration has brought new research interest [7,8].

Among many results, the transition to self-trapping is most interesting [9–13]. With increasing atomic interaction (repulsive), the Josephson oscillation between the two wells is blocked, and the atoms of a BEC in a symmetric double-well potential show a highly asymmetric distribution as if most atoms are trapped in one well. This phenomenon was observed in the laboratory recently [8].

In this paper we achieve insight into this somewhat counterintuitive phenomenon by addressing its underlying phase transition and the influence of many-body quantum fluctuations on the phase transition. Analytically we identify the self-trapping phenomenon as a continuous phase transition and the critical behavior is found to be characterized by a logarithm scaling law. We then extend our treatment to discuss many-body quantum fluctuation effects on self-trapping. We find that the transition point is shifted and the scaling law breaks down because of quantum fluctuations. Further investigations show that the quantum properties are quite different for different interaction regions, such as the self-trapping region and others. These properties can be well illustrated quantitatively using the entanglement entropy. By employing the average entropy as the order parameter, we can clearly demonstrate the quantum phase transition: The entanglement entropy reaches its maximum at the quantum transition point.

Our paper is organized as follows. In Sec. II, self-trapping is studied within the mean-field framework both analytically and numerically, revealing the critical behavior at the transition point. In Sec. III, we discuss the many-body quantum fluctuation effect and reveal the quantum entanglement manifestation of the transition to nonlinear self-trapping. Section IV contains our discussion and conclusion.

II. TRANSITION TO SELF-TRAPPING AND SCALING LAW

For two weakly coupled BECs trapped in a symmetric double well, the system can be described by the so-called two-mode Hamiltonian [3,14]

$$\hat{H} = \frac{\gamma}{2}(\hat{a}^\dagger\hat{a} - \hat{b}^\dagger\hat{b}) + \frac{c}{2N}(\hat{a}^\dagger\hat{a} - \hat{b}^\dagger\hat{b})^2 - \frac{v}{2}(\hat{a}^\dagger\hat{b} + \hat{b}^\dagger\hat{a}), \quad (1)$$

where the Bose operators $\hat{a}^{(\dagger)}$ and $\hat{b}^{(\dagger)}$ correspond to annihilation (creation) operators for the two wells, respectively, $\gamma = E_a^0 - E_b^0$ is the energy bias between the two wells, $E_i^0 = \int[(\hbar^2/2m)|\nabla\varphi_i|^2 + V(r)|\varphi_i|^2]dr$, $c = c_i = (4\pi\hbar aN/m)\int|\varphi_i|^4 dr$ denotes the effective interaction of atoms, $v = \int[(\hbar^2/2m)\nabla\varphi_a\nabla\varphi_b + V(r)\varphi_a\varphi_b]dr$ is the effective Rabi frequency which describes the coupling between two wells, N is the total atom number, which is conserved, a is the s-wave scattering length, and φ_i $(i=a,b)$ are the wave functions for each well. In the present work we focus on the case that has been realized in the laboratory recently. For this case, the potential is symmetric so that $\gamma=0$, and the interaction is repulsive, i.e., $c>0$.

If the particle number is large enough, the system can be well described in the mean-field approximation. In this approximation, the dynamics of the system is described by a classical Hamiltonian $H = \langle\Psi_{GP}|\hat{H}|\Psi_{GP}\rangle/N$ (up to a trivial constant) in which $|\Psi_{GP}\rangle = (1/\sqrt{N!})(a\hat{a}^\dagger + b\hat{b}^\dagger)^N|0\rangle$ is the

*Electronic address: Liu_Jie@iapcm.ac.cn

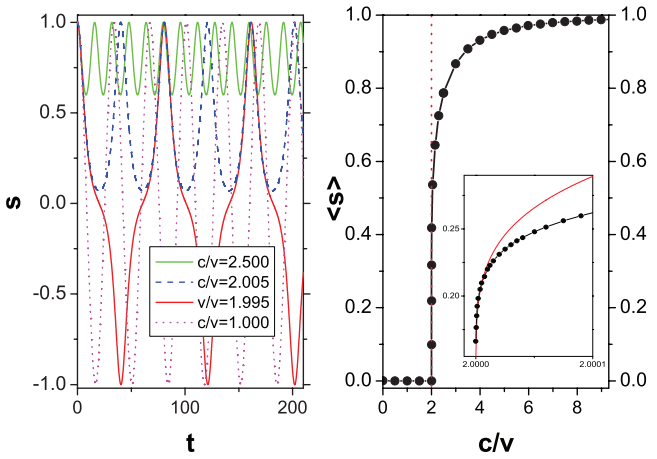

FIG. 1. (Color online) For initial condition $s=1$, the population difference evolves with time for $c/v=1, 1.995, 2.005, 2.5$ (left column), and the average population difference vs parameter c/v (right column). Inset: the critical behavior near $c/v=2$; the (red) line is for analytic formula (5) and the circles are for numerical simulation.

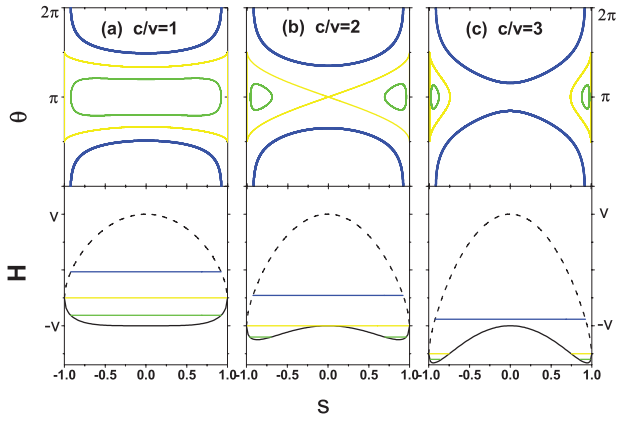

FIG. 2. (Color online) Trajectories on the phase space of the classical Hamiltonian system (2) (top panels). In the bottom panels we plot the energy profiles for the relative phase $\theta=0$ (dashed) and π (solid), respectively. The energies of the trajectories in the upper panels are also denoted in the bottom panels using the same style (color) of lines.

collective state of the N-particle system [3,14]. $a=|a|e^{i\theta_a}$ and $b=|b|e^{i\theta_b}$ are two c numbers which correspond to the probability amplitudes of atoms in the two wells. By introducing the population difference $s=|b|^2-|a|^2$ and the relative phase $\theta=\theta_b-\theta_a$, the classical Hamiltonian can be reduced to

$$H=-\frac{c}{2}s^2+v\sqrt{1-s^2}\cos\theta, \tag{2}$$

where s and θ are canonical conjugate coordinates. Their equations of motions are

$$\dot{s}=v\sqrt{1-s^2}\sin\theta, \quad \dot{\theta}=-cs-\frac{vs}{\sqrt{1-s^2}}\cos\theta. \tag{3}$$

The self-trapping motion occurs for trajectories whose average population difference is not zero $\langle s\rangle\neq 0$. In the experiment [8], all the atoms are placed initially in one well, i.e., $s(0)=1$ or -1. For small interaction, Josephson oscillation will be observed, and with larger interaction, the self-trapping emerges. This phenomenon can be well understood by the above classical Hamiltonian system (2). Figure 1 plots the evolution of the population difference s and its average for different interactions calculated by (3) with the initial condition $s(0)=1$. For c/v smaller than 2, the population difference oscillates symmetrically between 1 and -1, and its average is zero. However, for c/v larger than 2, the motion is limited in the half plane and the amplitude decreases with increasing interaction; hence, the average of the population difference will be nonzero and will increase with increasing interaction.

The above process can be well understood from on analysis on the phase space of the classical Hamiltonian system. In Fig. 2, we plot the trajectories in phase space and classical energy profiles for the different parameters. The (red) lines correspond to the trajectories when all the atoms are initially in one well, i.e., $s(0)=1$ or -1. From this figure, we can see clearly that the dynamical transition happens at the moment when the energy of the trajectory with initial condition $s(0)=1$ or -1, $H(s=\pm 1)=c/2$, equals the energy of the separatrix, which is $H=-v$. When the energy of the trajectory initially in one well is larger than $-v$, one finds only the Josephson oscillation trajectory, while for the energy smaller than $-v$, self-trapping happens.

For a classical Hamiltonian system we can obtain the period T of a given trajectory from the integral $T=\oint(\partial\theta/\partial H)ds$, and the average s for it from $\langle s\rangle=(1/T)\oint(\partial\theta/\partial H)s\,ds$, in which the integral path is along the trajectory. For the trajectory with initial condition $s(0)=\pm 1$, we have $H(s=\pm 1)=c/2$. Thus, from Eqs. (2) and (3), we get

$$T=\begin{cases} 2\displaystyle\int_{-1}^{1}\frac{ds}{v\sqrt{(1-s^2)-[c(1-s^2)/2v]^2}}, & c/v<2, \\ 2\displaystyle\int_{\sqrt{1-(2v/c)^2}}^{1}\frac{ds}{v\sqrt{(1-s^2)-[c(1-s^2)/2v]^2}}, & c/v>2, \end{cases} \tag{4}$$

and

$$\langle s\rangle=\begin{cases} \dfrac{2}{T}\displaystyle\int_{-1}^{1}\frac{s\,ds}{v\sqrt{(1-s^2)-[c(1-s^2)/2v]^2}}, & c/v<2, \\ \dfrac{2}{T}\displaystyle\int_{\sqrt{1-(2v/c)^2}}^{1}\frac{s\,ds}{v\sqrt{(1-s^2)-[c(1-s^2)/2v]^2}} & c/v>2, \end{cases} \tag{5}$$

in which we have used the formula $\cos\theta=c\sqrt{1-s^2}/2v$. After some elaboration, we obtain

$$\langle s\rangle = \begin{cases} 0, & c/v < 2, \\ \dfrac{\pm\pi\sqrt{(c/v)^2-4}}{(2c/v)\mathrm{Im}(K\{(c/v)^2/[(c/v)^2-4]\})}, & c/v > 2, \end{cases} \tag{6}$$

where $K(x)$ is the complete elliptic integral of the first kind. Near the transition point, it exhibits the logarithmic critical behavior

$$\langle s\rangle \approx \pm\frac{\sqrt{2}\pi}{(c/v)\ln[(c/v)^2-4]}. \tag{7}$$

The inset of Fig. 1 plots this critical behavior, where the theoretical results is confirmed by numerical results obtained by numerically solving Eq. (3) with the fourth- and fifth-order step-adaptive Runge-Kutta algorithm.

Our logarithmic critical behavior is very similar to the critical behavior in the measure synchronization in coupled Hamiltonian systems [15]. This is because critical behavior in both cases is closely related to the separatrix of the Hamiltonian. Near the separatrix the period of the trajectory diverges to infinity; as a function of the relative deviation of the energy from the separatrix energy, its divergency follows a logarithmic law [16].

In the above discussion, the initial state is set as $s=1$; in fact for any initial state denoted by s_i, θ_i the transition to self-trapping occurs at some interaction parameter, and the critical behavior follows the same logarithmic behavior. If we extend the above discussion to this general case, we can obtain the general criterion for the occurrence of self-trapping, i.e., $H(s_i,\theta_i,c,v)<-v$. Then the critical point is expressed as

$$\left(\frac{c}{v}\right)_{cr} = 2(1+\sqrt{1-s_i^2}\cos\theta_i)/s_i^2. \tag{8}$$

From the above analytic expression, we see that an initial state with smaller population difference requires stronger nonlinearity so that self-trapping occurs. Moreover, the critical point can be adjusted by the relative phase between the two weakly linked BECs in the double well. For example, for the case when the population difference is 0.5, the critical point approximates to 15 and 8 for $\theta_i=0$ and $\pi/2$, respectively. In practical experiments, the relative phase can be adjusted by using a "phase-imprinting" method, i.e., shining on uniform laser light on the BECs in a double well. This method has been successfully applied to generate dark solitons in cigar-shaped BECs [17].

III. MANY-BODY QUANTUM FLUCTUATION EFFECTS

In the mean-field treatment we assume that the number of particle is large. However, in practical experiments, the particle number is finite. In order to understand the quantum fluctuation effect due to finite particle number, we should investigate the self-trapping within the framework of the many-body quantum system (1) [18,19].

In treating the quantum many-body problem it is helpful to bear in mind some results from quantum-information theory concerning entanglement [20]. Quantum entanglement is realized to be not only a crucial resource that allows for powerful communication and computational tasks that are not possible classically, but also a signal of quantum long-range correlation; therefore it can serve as an indicator of a quantum transition in a real solid system [21]. Recent years have witnessed growing interest in studying the interplay between entanglement and the quantum phase transition [22–26].

Previously, some efforts have been devoted to studying the dynamics of BECs in double wells using a full quantum treatment [27,28]. In Ref. [27] the authors presented a quantum phase-space model of BECs in a double-well potential by using the Husimi distribution function. They showed a good correspondence between the phase space of the classical Hamiltonian (2) (mean-field approximation) and the quantum phase space of the two-mode Hamiltonian (1) (full quantum framework). The authors of Ref. [28] calculated the time evolutions of states and their corresponding entanglement with different initial states for several different interactions between atoms. The time evolutions of entanglement entropy presented in Ref. [28] for several interactions between atoms show a tendency to decrease with increasing interactions.

In our following discussions in this section, however, we focus on the critical behavior at the transition to self-trapping as revealed by the above discussions, addressing how the quantum fluctuations influence the transition behavior. As will be shown later, the transition point is shifted and the scaling law breaks down due to the quantum fluctuations. With increasing atom number, the transition behavior demonstrates a perfect classical-quantum correspondence. We also calculate the entanglement entropy, achieving insight into the quantum transition. Our calculations on the time evolution of the entanglement entropy confirm the results of [28], and our further calculations on the time-averaged entanglement strongly suggest that the entanglement entropy of this system serves as a good order parameter to describe such a quantum transition.

A. Quantum phase transition

In the quantum framework the evolution of the system is governed by the Schrödinger equation

$$i\frac{d}{dt}|\psi(t)\rangle = \hat{H}|\psi(t)\rangle, \tag{9}$$

where $|\psi(t)\rangle=\Sigma_{n=0}^{N}a_n|n,N-n\rangle$,

$$|n,N-n\rangle = [1/\sqrt{n!(N-n)!}](\hat{a}^\dagger)^n(\hat{b}^\dagger)^{N-n}|0\rangle$$

$(n=0,\ldots,N)$ are Fock states, and a_n are the probability amplitudes. Hence, the population difference is given by

$$s = \sum\frac{|a_n|^2(N-2n)}{N}. \tag{10}$$

We choose $|0,N\rangle$ as the initial state in the full quantum framework, which corresponds to $s=1$ in the mean-field model. In Fig. 3, we plot the average population difference

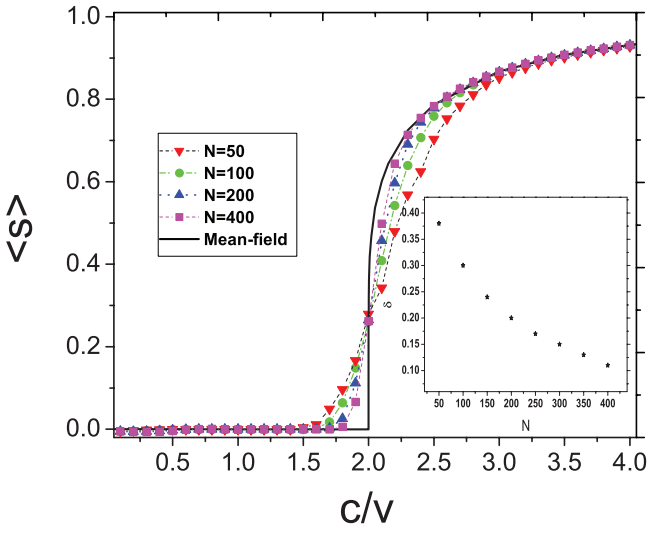

FIG. 3. (Color online) The average of the population difference vs the parameter c/v obtained by full quantum simulations. Here, the initial state is $(n=0,\ldots,N)$, namely, $s=1$. Inset: The shift of the critical point compared with the mean-field prediction δ for different atom numbers.

calculated from the above Schrödinger equation for different total particle numbers. From the above calculation, we find that the quantum fluctuation has two significant effects on the transition to self-trapping. First, the critical point is shifted to the left-hand side due to the finiteness of the particle number. From Fig. 3, it is clearly seen that, if the parameters c, v are kept constant, with increasing number of atoms, the transition point clearly shifts to the left. For example, for $N=50$, the transition point shifts to $c/v=1.6$. We know that the quantum fluctuation is closely relatesd to the effective Planck constant; here for this model it is $\frac{2}{N}$ [29]. Therefore we expect that the deviation from the mean-field critical point should be inversely proportional to the total atom number. This prediction is confirmed by our calculations as shown in the inset of Fig. 3, in which δ is the difference between the quantum transition point and the mean-field one.

Second, the logarithm scaling law breaks down because of the quantum fluctuations. In Fig. 3 we find that quantum fluctuations destroy the logarithm scaling law of the mean field and no clear scaling law is observed for the quantum case. With increasing atom number the quantum results tends to the mean-field results in the limit $N\to\infty$, as required by the classical-quantum correspondence principle [29].

We should note that in the above calculation the time period for the average should be much longer than the period of the fastest oscillations but shorter than the period of the shortest quantum beating. This is because, essentially, the dynamics of the quantum system is periodic or quasiperiodic; therefore, any dynamical effects of the quantum system depend on the time scales [18,30]. In our problem, there are two time scales, one for integrating the classical equation (3) and the other for integrating the quantum equation (10). The latter is N times the former. In our calculations, the average time is $50N$, meaning that the corresponding classical time scale is the same (=50). On the other hand, we find that, the

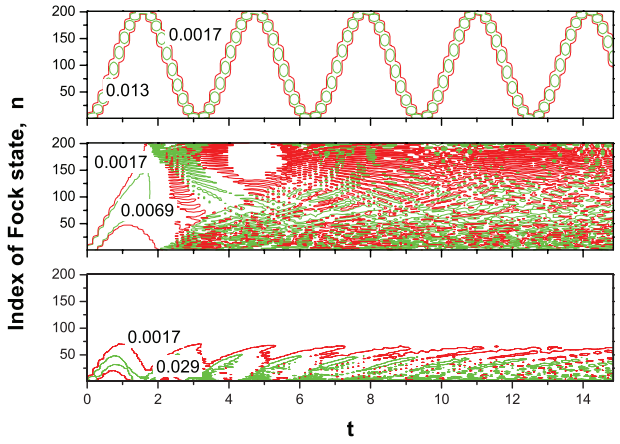

FIG. 4. (Color online) Occupations of Fock states for different times. The contours denote the probabilities of occupations. From top to bottom, $c/v=0,1.995,2.5$, respectively.

averaged population difference increases gradually to 0.001 and then rises quickly. This is different from the mean-field situation, where the averaged population difference stays at zero and then becomes nonzero after the critical point. So, in the quantum case, we define the transition point as the point where the averaged population difference is larger than 0.001. This observation also suggests that there is no scaling law for the finite-particle situation.

B. Entanglement manifestation of the quantum phase transition

To well understand the self-trapping phenomenon in the full quantum description, we calculate the evolution of the occupation of Fock states $|n,N-n\rangle$ $(n=0,\ldots,N)$. Figure 4 shows the evolution of the Fock state occupation for different interactions. The horizontal axis is the time t; the vertical axis is the index of the Fock state, namely, n corresponds to $|n,N-n\rangle$, and the contour is for the occupation probability. Figure 4(a) is for the linear case, which shows that the occupations are oscillating between $|0,N\rangle$ and $|N,0\rangle$. For $c=1.95$ [see Fig. 4(b)], near the transition point, we see that the wave function spreads much more rapidly to all the Fock states. Figure 4(c) is plotted for the self-trapping case, $c=2.5$, from which we see that the occupation distributed is narrowed in partial Fock states, so that the average of the population difference is nonzero.

From Fig. 4, we also see that the dynamics properties of such a quantum system are quite different for different interaction regions. To achieve more insight into the quantum transition to self-trapping, we introduce the quantum entanglement entropy. For the system with the wave function $|\psi\rangle=\Sigma_{n=0}^{N}a_n|n,N-n\rangle$, the density operator is given by

$$\rho=|\psi\rangle\langle\psi|=\sum_{n,m}a_n a_m^*|n,N-n\rangle\langle N-m,m|. \tag{11}$$

Taking the partial trace with respect to one well yields the reduced density operator for the other,

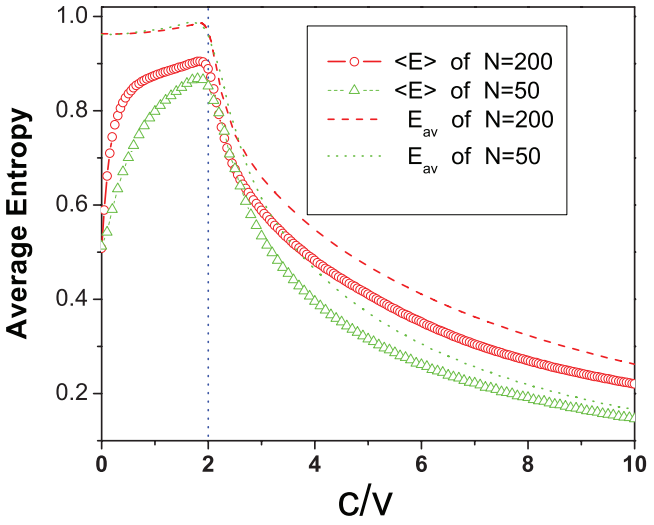

FIG. 5. (Color online) The entanglement entropy for different c/v. The line with circles is for E_{av} and the dashed line for $\langle E\rangle$.

$$\rho_a = \sum_n |a_n|^2 |n\rangle\langle n|. \tag{12}$$

Thus, the entropy of entanglement between the two coupled BEC's is given by [19]

$$E(\rho) = -\sum_{n=0}^{N} |a_n|^2 \log_2 |a_n|^2. \tag{13}$$

The entanglement entropy has the following properties: its reaches its maximum $E(\rho)=\log_2 N$ when $|a_n|^2=1/N$, and its minimum $E(\rho)=0$ when $|a_n|^2=1$ and the others parameters are zero.

Because the self-trapping is a dynamic phenomenon, the occupation of each Fock state varies in time; therefore, we use the average entropy. Technically, we have two choices to average it: we can average the occupation first and then calculate the entropy, or calculate the entropy first then average it. So we denote

$$E_{av} = -\sum_{n=0}^{N} \langle |a_n|^2\rangle \log_2 \langle |a_n|^2\rangle / \log_2 N \tag{14}$$

and

$$\langle E\rangle = \left\langle -\sum_{n=0}^{N} |a_n|^2 \log_2 |a_n|^2 \right\rangle \Big/ \log_2 N. \tag{15}$$

The above formulas have been normalized by $\log_2 N$.

In Fig. 5, we plot the two kinds of average entropy with different interactions. Obviously, the dynamics of the quantum system can be well illustrated by the average entropies of quantities. For the linear case, the atoms mainly occupy several Fock states at a given time [see Fig. 4(a)], and the occupied states change with time. Thus, the instantaneous entropy is small; and so is the average entropy $\langle E\rangle$. On the other hand, because the average populations of each Fock state are almost equivalent for this case, E_{av} should be large. With increasing interaction, the occupations in Fock states extend so that the instantaneous entropy increases. However, when the interaction exceeds the transition point self-trapping occurs and the occupations are limited to several Fock states [see Fig. 4(c)]; hence, the instantaneous entropy becomes small and so does $\langle E\rangle$. For the same reason E_{av} will be small for self-trapping cases. From Fig. 5, we also observe that E_{av} is almost independence of the particle number and varies very little with changing interaction parameter before it reaches its maximum. After that, it becomes quite sensitive to the particle number as well as the interaction parameter. However, the entropy $\langle E\rangle$ before and after the maximum point shows strong dependence on the particle number.

It is interesting that the two average entropies reach their maxima at a point very close to the transition point of the mean field, $c/v=2$. This is very similar to phase transitions of spin systems, where the phase transition happens at the point when the entanglement of the system reaches its maximum [24]. This is different from the situation of the two-impurity Kondo model where the entanglement vanishes at a quantum critical point [25]. In particular, we find that the maximum points of the average entropies vary very little with changing particle number. This property suggests that the entanglement entropy is a better quantity than the average population to serve as the indicator of a quantum phase transition, because the latter is too sensitive to the particle number as shown in Fig. 3.

IV. DISCUSSION AND CONCLUSION

In conclusion, we have made a thorough analysis of the transition to self-trapping for BECs confined in a symmetric double well. Analytically we identify it as a continuous phase transition, where the time-averaged population difference between two wells changes from zero to nonzero following a logarithmic law at the critical point. We also discuss the influence of many-body quantum fluctuations on the transition to self-trapping. We find that the transition point is significantly shifted by quantum fluctuations and no scaling law is observed in the quantum description. We investigate the quantum entanglement manifestation of the transition and find that the entanglement entropy reaches its maximum at the transition point. The classical-quantum correspondence in the transition process is discussed.

ACKNOWLEDGMENTS

This work was supported by the National Natural Science Foundation of China (Grant No. 10474008, and No. 10604009), the Science and Technology fund of CAEP, the National Fundamental Research Program of China under Grant No. 2005CB3724503, and the National High Technology Research and Development Program of China (863 Program) international cooperation program under Grant No. 2004AA1Z1220. We thank Y. Ma for her help in some calculations.

[1] M. Grifoni and P. Hänggi, Phys. Rep. **304**, 229 (1998).
[2] M. H. Anderson, J. R. Ensher, M. R. Matthews, C. E. Wieman, and E. A. Cornell, Science **269**, 198 (1995); K. B. Davis, M.-O. Mewes, M. R. Andrews, N. J. van Druten, D. S. Durfee, D. M. Kurn, and W. Ketterle, Phys. Rev. Lett. **75**, 3969 (1995); C. C. Bradley, C. A. Sackett, J. J. Tollett, and R. G. Hulet, *ibid.* **75**, 1687 (1995).
[3] Franco Dalfovo, Stefano Giorgini, L. P. Pitaevskii, and S. Stringari, Rev. Mod. Phys. **71**, 463 (1999); Anthony J. Leggett, *ibid.* **73**, 307 (2001), and references therein.
[4] O. Zobay and B. M. Garraway, Phys. Rev. A **61**, 033603 (2000); Biao Wu and Qian Niu, *ibid.* **61**, 023402 (2000); F. Kh. Abdullaev and R. A. Kraenkel, *ibid.* **62**, 023613 (2000); F. Meier and W. Zwerger, *ibid.* **64**, 033610 (2001).
[5] Jie Liu, Biao Wu, and Qian Niu, Phys. Rev. Lett. **90**, 170404 (2003); Jie Liu *et al.*,Phys. Rev. A **66**, 023404 (2002).
[6] S. Giovanazzi *et al.*, Phys. Rev. Lett. **84**, (2000) 4521; Li-Bin Fu, Jie Liu, and Shi Gang Chen, Phys. Lett. A **298**, 388 (2002).
[7] Y. Shin, M. Saba, T. A. Pasquini, W. Ketterle, D. E. Pritchard, and A. E. Leanhardt, Phys. Rev. Lett. **92**, 050405 (2004).
[8] M. Albiez, R. Gati, Jonas Fölling, S. Hunsmann, M. Cristiani, and M. K. Oberthaler, Phys. Rev. Lett. **95**, 010402 (2005).
[9] G. J. Milburn *et al.*, Phys. Rev. A **55**, 4318 (1997).
[10] A. Smerzi, S. Fantoni, S. Giovanazzi, and S. R. Shenoy, Phys. Rev. Lett. **79**, 4950 (1997).
[11] S. Raghavan, A. Smerzi, and V. M. Kenkre, Phys. Rev. A **60**, R1787 (1999).
[12] S. Raghavan, A. Smerzi, S. Fantoni, and S. R. Shenoy, Phys. Rev. A **59**, 620 (1999).
[13] Sigmund Kohler and Fernando Sols, Phys. Rev. Lett. **89**, 060403 (2002); L. Salasnich, Phys. Rev. A **61**, 015601 (2000).
[14] M. J. Steel and M. J. Collett, Phys. Rev. A **57**, 2920 (1998); J. I. Cirac, M. Lewenstein, K. Molmer, and P. Zoller, *ibid.* **57**, 1208 (1998).
[15] A. Hampton and D. H. Zanette, Phys. Rev. Lett. **83**, 2179 (1999).
[16] A. J. Lichtenberg and M. A. Lieberman, *Regular and Chaotic Dynamics*, 2nd ed. (Springer-Verlag Berlin 1983).
[17] Biao Wu, Jie Liu, and Qian Niu Phys. Rev. Lett. **88**, 034101 (2002).
[18] S. Raghavan, A. Smerzi, and V. M. Kenkre, Phys. Rev. A **60**, R1787 (1999).
[19] Andrew P. Hines, Ross H. McKenzie, and Gerard J. Milburn, Phys. Rev. A **67**, 013609 (2003).
[20] A. Galindo and M. A. Martin-Delgado, Rev. Mod. Phys. **74**, 347 (2002).
[21] T. J. Osborne and M. A. Nielsen, Phys. Rev. A **66**, 032110 (2002); A. Osterloh, L. Amico, G. Falci, and R. Fazio, Nature (London) **416**, 608 (2002).
[22] F. Verstraete, M. A. Martin-Delgado, and J. I. Cirac, Phys. Rev. Lett. **92**, 087201 (2004); J. J. Garcia-Ripoll, M. A. Martin-Delgado, and J. I. Cirac, *ibid.* **93**, 250405 (2004).
[23] J. Vidal, R. Mosseri, and J. Dukelsky, Phys. Rev. A **69**, 054101 (2004); J. Vidal, Guillaume Palacios, Phys. Rev. A **70**, 062304 (2004).
[24] Shi-Jian Gu, Shu-Sa Deng, You-Quan Li, and Hai-Qing Lin, Phys. Rev. Lett. **93**, 086402 (2004); Shi-Jian Gu, Guang-Shan Tian, and Hai-Qing Lin, Phys. Rev. A **71**, 052322 (2005).
[25] C. Brukner, V. Vedral, and A. Zeilinger, Phys. Rev. A **73**, 012110 (2006); S. Y. Cho and R. H. McKenzie, *ibid.* **73**, 012109 (2006).
[26] Yan Chen, Z. D. Wang, and F. C. Zhang, Phys. Rev. B **73**, 224414 (2006).
[27] K. W. Mahmud, H. Perry, and W. P. Reinhardt, Phys. Rev. A **71**, 023615 (2005).
[28] A. P. Tonel, J. Links, and A. Foerster, J. Phys. A **38**, 1235 (2005).
[29] Biao Wu and Jie Liu, Phys. Rev. Lett. **96**, 020405 (2006).
[30] V. M. Kenkre, Jϕrgensen, and P. L. Christiansen, Physica D, **90**, 280 (1996).